ANL-6587

ANL-6587

Argonne National Laboratory

PHYSICS ANALYSIS OF THE JUGGERNAUT REACTOR

by

D. P. Moon

ANL-6587
Reactor Technology
(TID-4500, 17th Ed.)
AEC Research and
Development Report

ARGONNE NATIONAL LABORATORY
9700 South Cass Avenue
Argonne, Illinois

PHYSICS ANALYSIS OF THE JUGGERNAUT REACTOR

by

D. P. Moon

Reactor Engineering Division

July 1962

Operated by The University of Chicago
under
Contract W-31-109-eng-38

TABLE OF CONTENTS

	Page
LIST OF SYMBOLS	5
I. INTRODUCTION	7
II. CRITICAL ASSEMBLY - THE ARGONAUT	8
Experimental Data	8
Two-group Constants	9
Criticality Study	10
III. THE JUGGERNAUT REACTOR	12
Core Design	12
Two-group Constants	15
Adjoint and Real Fluxes	16
Perturbation Calculations	21
Criticality Study	32
Control System Design	35
Experimental Data	38
IV. APPENDIX A - Optimum Size of the Internal Thermal Column	41
V. APPENDIX B - Computation of Adjoint Fluxes Using PDQ	45
ACKNOWLEDGEMENT	46
REFERENCES	47

LIST OF FIGURES

No.	Title	Page
1.	JUGGERNAUT Fuel Assembly	13
2.	Core Arrangement	14
3.	Idealized Reactor Structure	15
4.	Thermal-neutron Flux at 100 kw with All Control Rods Withdrawn.	17
5.	Fast-neutron Flux at 100 kw with All Control Rods Withdrawn.	18
6.	Two-group Thermal Adjoint Flux with All Control Rods Withdrawn.	19
7.	Two-group Adjoint Flux with All Control Rods Withdrawn.	20
8.	Thermal-neutron Flux as a Function of Radial Position at Core Midplane	20
9.	Thermal-neutron Flux as a Function of Axial Position for Core and Internal Thermal Column	21
10.	Comparison of Thermal Adjoint Flux Shapes with and without Al-H_2O Shells Surrounding the Core.	24
11.	Local Void Coefficients of Reactivity	25
12.	Variation in Reactivity with H:U^{235} Ratio as Effected by Number of Plates per Assembly	33
13.	Worth of Cylindrical Cd Shell as a Function of Shell Height	36
14.	Worth of Control Rod System Relative to Cadmium Shell	36
15.	Optimum Radii of Graphite Internal Thermal Columns	44

LIST OF TABLES

No.	Title	Page
1.	Experimental Data - ARGONAUT Reactor	8
2.	Two-group Constants for the ARGONAUT One-slab Configuration	9
3.	Two-group Constants for the ARGONAUT Annular Configuration	10
4.	Corrections to Two-group Constants Used for the One-slab Calculation	11
5.	JUGGERNAUT Two-group Constants	16
6.	Core Importance Functions for Standard Operating Reactor	23
7.	Core Importance Functions for Cold Clean Critical Reactor	24
8.	Changes in Two-group Constants for Temperature Rise of 45°C	25
9.	Changes in Two-group Constants for 10% Distributed Voids	26
10.	Xenon Poisoning Analysis	27
11.	Constants for Homogenized Shells	29
12.	Changes in Two-group Constants Assuming Radial Fuel-Plate Arrangement	30
13.	Changes in Two-group Constants Resulting from U^{235} Movement from Edges Toward Core Center	31
14.	Summary of Calculated Perturbation Effects	32
15.	Variation in Core Properties for Different Plate Spacings	33
16.	Summary of Reactor Parameters	38
17.	Excess Reactivity Requirements	39

LIST OF SYMBOLS

B_m^2	Two-group buckling (cm^{-2})
D_1	Two-group fast diffusion coefficient (cm)
D_2	Two-group thermal diffusion coefficient (cm)
E_c	Cut-off energy for thermal neutrons (ev)
f_x	Volume fraction of material x
ϕ_1	Two-group fast flux [$n/(cm^2)(sec)$]
ϕ_2	Two-group thermal flux [$n/(cm^2)(sec)$]
ϕ_1^+	Two-group fast adjoint flux
ϕ_2^+	Two-group thermal adjoint flux
k_∞	Infinite multiplication factor
$\Delta k/k'$	Reactivity change
ℓ	Prompt neutron lifetime (sec)
L^2	Thermal diffusion area (cm^2)
λ	Eigenvalue from PDQ printout ($\approx k_{eff}$)
λ_{Xe}	Xenon decay constant (sec^{-1})
ν	Average number of neutrons released per thermal fission
ρ	Reactivity
Σ_1	Two-group fast removal cross section (cm^{-1})
Σ_a	Two-group thermal absorption cross section (cm^{-1})
Σ_f	Two-group thermal fission cross section (cm^{-1})
T_M	Moderator temperature (°C or °K)
T_N	Neutron temperature (°C or °K)
τ_1	Neutron age for fast group of 3-group system (cm^2)
τ_2	Neutron age for intermediate group of 3-group system (cm^2)
τ_f	Neutron age for fast group of 2-group system (cm^2)
V	Volume
$W_{U^{25}}$	Mass of U^{235} within reactor or critical mass of U^{235}
y	Primary fission product yield

PHYSICS ANALYSIS OF THE JUGGERNAUT REACTOR

by

D. P. Moon

I. INTRODUCTION

The JUGGERNAUT is an intermediate-power research reactor, designed and constructed at Argonne National Laboratory as a supporting facility for chemistry and physics research. It is designed to provide thermal-neutron fluxes up to 4×10^{12} n/(cm^2)(sec) at an operating power of 250 kw.

The design of the JUGGERNAUT closely resembles that of the ARGONAUT, which is a versatile, low-power reactor designed for use as a training facility and for the conduct of experiments in reactor physics. Both reactors contain a graphite, internal thermal column surrounded by a water-cooled fuel annulus which is in turn surrounded by graphite. The apparent differences are in the diameter of the internal thermal column, which is 46 cm for the JUGGERNAUT but 61 cm for the ARGONAUT, and in the fuel-plate arrangement. In the ARGONAUT, the plates are placed perpendicular to the radial direction and contained in 24 assemblies; graphite fillers are used between assemblies. In the JUGGERNAUT annulus, the plates are arranged along radial planes and contained in 20 assemblies; no graphite fillers are necessary.

Since the design of the JUGGERNAUT is similar to that of the ARGONAUT, the physics analysis of the JUGGERNAUT was checked using the ARGONAUT as a "critical assembly." Those methods of evaluating the nuclear characteristics of the ARGONAUT which gave good agreement with experimental data were considered to be applicable to the analysis of the JUGGERNAUT.

The analyses for both the JUGGERNAUT and the ARGONAUT were based on a modified two-group theory. The criticality calculations were carried out with the IBM-704 and the two-dimensional PDQ code. Reactivity effects were calculated by hand by means of perturbation techniques, with the real and adjoint fluxes obtained from PDQ calculations.

The more important design criteria for the JUGGERNAUT were: (1) the reactor must be inherently self-limiting for rapid insertion of a large amount of reactivity (~3% Δk); (2) rapid insertion of greater amounts of reactivity than the reactor can handle safely must be impossible without

major reactor alterations or circumvention of procedures and interlocks; (3) the thermal-neutron flux is to be as high as possible consistent with other design objectives; (4) adequate experimental space must be provided; (5) the reactor is to be completed for a low total cost.

II. CRITICAL ASSEMBLY - THE ARGONAUT

Experimental Data

The ARGONAUT has a more versatile fuel-loading pattern than does the JUGGERNAUT. The fuel plates can be arranged in at least 6 different configurations within a 15-cm-wide annulus. The ARGONAUT annular loading has the greatest similarity to the JUGGERNAUT fuel configuration; however, the other ARGONAUT configurations are also of interest in order to ensure that the physics analysis has general validity.

A certain amount of the data contained in the ARGONAUT log books has been compiled and is available as the "Argonaut Reactor Data Book."[1] Other information is available in various reports.[2-4] Some data of interest for the several configurations are given in Table 1.

Table 1

EXPERIMENT DATA - ARGONAUT REACTOR

Property	Annular	One Slab	Two Slab
Critical Mass* (U^{235}), kg	3.99	1.87→1.99	3.5→3.8
Worth of Top Reflector, % $\Delta k/k$	-	0.8	0.3
Worth of Cadmium at Core-Reflector (midplane), % $(\Delta k/k)/cm^2$	-	-0.003	-
Temperature Coefficient of Reactivity (55°C), % $(\Delta k/k)/°C$	-0.0155	-	-0.020
Average Void Coefficient of Reactivity (20°C), % $(\Delta k/k)/1\%$ void	-	-0.20	-

*The critical mass varies with the arrangement of fuel plates for any one configuration. In most cases, the fuel was more concentrated in zones of higher statistical weight, thus reducing the critical mass. The 2 values for the one-slab loading give an indication of the magnitude of this effect. A critical mass of 1.87 kg was obtained with a high concentration of fuel in the central fuel boxes, whereas a critical mass of 1.99 kg was obtained with the higher concentration in the outermost fuel boxes.[2]

Two-group Constants

The method of obtaining two-group constants for the ARGONAUT can be briefly described as follows: Deutsch's 3-group constants[5] were reduced to 2 groups upon consideration of leakage effects for the equivalent bare reactor. In the slab configuration, the definition of the equivalent bare reactor was the standard one, although for the annular or more complicated configuration the "equivalent bare reactor" was defined as a bare homogeneous cylindrical reactor, with the same material constants as the ARGONAUT core, of just critical dimensions and with no internal thermal column. It was required that the same criticality solution be obtained by 2-group theory as by 3-group theory for the equivalent bare reactor. The reason for this stress on 3-group theory is the fact that a convolution of 2 diffusion kernels gives a better representation of the experimental slowing-down density in water than does the single diffusion kernel of 2-group theory. Four or more groups would be even better, but were not used because of the resulting sacrifice in simplicity.

The details of this method and the results for the one-slab and annular configurations are given at length elsewhere.[2] Summaries of the nuclear constants are included here as Tables 2 and 3.

Table 2

TWO-GROUP CONSTANTS FOR THE ARGONAUT
ONE-SLAB CONFIGURATION

Core			
T_M = 20°C		Σ_1 = 0.0212 cm^{-1}	
T_N = 49°C		Σ_a = 0.013545 + 0.025273 $W_{U^{235}}$ cm^{-1}	
E_c = 0.18 ev		$\nu\Sigma_f$ = 0.0518305 $W_{U^{235}}$ cm^{-1}	
τ_1 = 38.23 cm^2		$L^2 = \frac{1}{0.064073 + 0.11955\ W_{U^{235}}}$	
τ_2 = 17.19 cm^2		D_1 = 1.30 cm	
τ_f = 61.3 cm^2		D_2 = 0.211 cm	
B_m^2 = 0.0090 cm^{-2}			
Graphite		**Vertical Reflector, H_2O**	
L^2 = 1700 cm^2		L^2 = 7.510 cm^2	
τ_f = 385 cm^2		τ_f = 31.8 cm^2	
D_1 = 1.14 cm		D_1 = 1.20 cm	
D_2 = 0.916 cm		D_2 = 0.1435 cm	
Σ_a = 0.000539 cm		Σ_a = 0.0191 cm^{-1}	

These constants assume a homogenized core and employ the 1958 World consistent set of cross sections.[6]

Table 3

TWO-GROUP CONSTANTS FOR THE ARGONAUT ANNULAR CONFIGURATION

Core

$T_M = 20°C$	$\Sigma_1 = 0.022364\ cm^{-1}$
$T_N = 40°C$	$\Sigma_a = 0.014701 + 0.016226\ W_{U^{25}}\ cm^{-1}$
$\tau_1 = 36.38\ cm^2$	$\nu\Sigma_f = 0.033223\ W_{U^{25}}\ cm^{-1}$
$\tau_2 = 16.19\ cm^2$	$L^2 = 2.657\ cm^2\ (W_{U^{25}} = 4.0\ kg)$
$\tau_f = 58.8\ cm^2$	$D_1 = 1.315\ cm$
$B_m^2 = 0.010513\ cm^{-2}$	$D_2 = 0.212\ cm$

Graphite

$\tau_f = 385\ cm^2$	
$D_1 = 1.14\ cm$	
$D_2 = 0.916\ cm$	
$\Sigma_1 = 0.002961\ cm^{-1}$	
$\Sigma_a = 0.000539\ cm^{-1}$	

Vertical Reflector, H_2O

$\tau_f = 31.8\ cm^2$	
$D_1 = 1.20\ cm$	
$D_2 = 0.142\ cm$	
$\Sigma_1 = 0.0374\ cm^{-1}$	
$\Sigma_a = 0.0195\ cm^{-1}$	

Concrete

$\tau_f = 205\ cm^2$	
$D_1 = 1.51\ cm$	
$D_2 = 0.707\ cm$	
$\Sigma_1 = 0.00737\ cm^{-1}$	
$\Sigma_a = 0.00736\ cm^{-1}$	

Reflector Outside Graphite

$\tau_f = 140\ cm^2$	
$D_1 = 1.37\ cm$	
$D_2 = 0.439\ cm$	
$\Sigma_1 = 0.00979\ cm^{-1}$	
$\Sigma_a = 0.00822\ cm^{-1}$	

These constants assume a homogenized core and employ the 1959 World consistent set of cross sections.(7)

Criticality Study

One-slab Configuration

The value for the critical mass of the one-slab configuration was obtained from a PDQ calculation in which the curvature of the slab was closely reproduced by a series of rectangular steps.(2) Some of the constants used in this calculation were slightly different from the corrected values given in Table 2. These discrepancies are listed in Table 4.

Table 4

CORRECTIONS TO TWO-GROUP CONSTANTS USED FOR ONE-SLAB CALCULATION

Constant	Value Used	Corrected Value
$D_{1_{core}}$	1.29 cm	1.30 cm
$\Sigma_{1_{core}}$	0.0233 cm^{-1}	0.0212 cm^{-1}
$D_{1_{graphite}}$	1.11 cm	1.14 cm

If the corrected values are used, all changes are in the direction of decreased reactivity or increased critical mass. It is estimated[8] that the changes in D_1 in the core and reflector would decrease the reactivity 0.3%, equivalent to 30 gm of U^{235}.[2] The change in Σ_1 for the core is equivalent to a change in τ_{core} from 55.4 cm^2 to 61.3 cm^2. The quantity $[\partial W_{U^{25}}/\partial \tau_{f(core)}]_{D_{1c}}$ has been calculated to be 0.0333 kg/cm^2 for $\tau_{f(core)}$ in the range from 55 to 60 cm^2. Hence, the critical mass obtained with the corrected constants would be 0.23 kg greater than that calculated. The calculated critical mass was 1.86 kg; hence, the corrected critical mass is 2.09 kg. The accepted experimental critical mass is 1.93 kg; however, this was obtained with a higher concentration of U^{235} in regions of greater importance (i.e., dummy fuel plates were used at the convex face of the core). Hence the calculation, which assumes uniform distribution of the fuel, would give a fictitiously high critical mass. Other perturbation effects have also been neglected. Inclusion of all these effects produces agreement between the calculation and experiment to within 1% in reactivity.

Annular Configuration

The constants used for the annular calculation are those listed in Table 3, with $W_{U^{25}}$ assumed to be 4.0 kg. An excess reactivity of 2.0% Δk was obtained. Most of this excess reactivity can be attributed to neglect of the negative reactivity effects caused by the aluminum containers, thin layers of H_2O at the core-reflector interface, and control plate voids. The fuel was distributed approximately uniformly in the experiment. Agreement between the calculation and experiment is obtained to within 1% in reactivity if the perturbation effects are taken into consideration.

III. THE JUGGERNAUT REACTOR

Core Design

For a power-limited reactor of the JUGGERNAUT type, the highest thermal-neutron flux within the internal thermal column would be obtained with an internal thermal column (ITC) of 30-cm diameter.* The JUGGERNAUT, however, uses a column of larger diameter (45.7 cm) in order to provide a greater amount of experimental space in high-flux regions. A still larger column would possibly be necessary if lattice studies had been planned for the internal region. For the 46-cm-diameter column, the reduction in the thermal flux from its value for the optimum diameter should be less than 9%.

The internal thermal column is surrounded by an annular core with an "active" width and height of 7.302 cm and 57.15 cm, respectively. The active core is surrounded on all sides, first, by a thin Al-H_2O region, and then by a graphite reflector in the radial direction, and by an H_2O reflector in the vertical direction.

Plate-type fuel is arranged in a radial pattern within the fuel annulus (see Figs. 1 and 2). The radial arrangement provides an almost uniform fuel density, hence eliminating the need for graphite fillers as used in the ARGONAUT. It also provides adequate shutdown cooling by radiative transfer alone, and provides an ideally symmetric lattice for the measurement of the effective delayed-neutron fraction (β_{eff}) by the poison-substitution method.

The thickness and spacing of fuel plate were selected to combine rigidity of structure with a large negative void coefficient, without departing significantly from a condition of minimum critical mass. Additional restraints on the design were: (1) the necessity of providing adequate cooling area, and (2) the necessity of providing a plate spacing which ensures a self-limiting response to nuclear excursions prompted by large reactivity inputs.

A suitable compromise involves 0.178-cm-thick plates, spaced 0.5205 cm apart to allow a total of 240 plates to be loaded into the core. The maximum possible fuel loading is 4.2 kg of U^{235} (170 plates/16.7 gm per plate and 70 plates/20 gm per plate), which was calculated to provide an excess reactivity of 6.5% Δk over the clean cold critical condition (3.3 kg). If necessary, more fuel plates can be fitted into the core by reducing the plate spacing. This is done through a simple swaging operation of the aluminum buttons which separate the plates.

*See Appendix A.

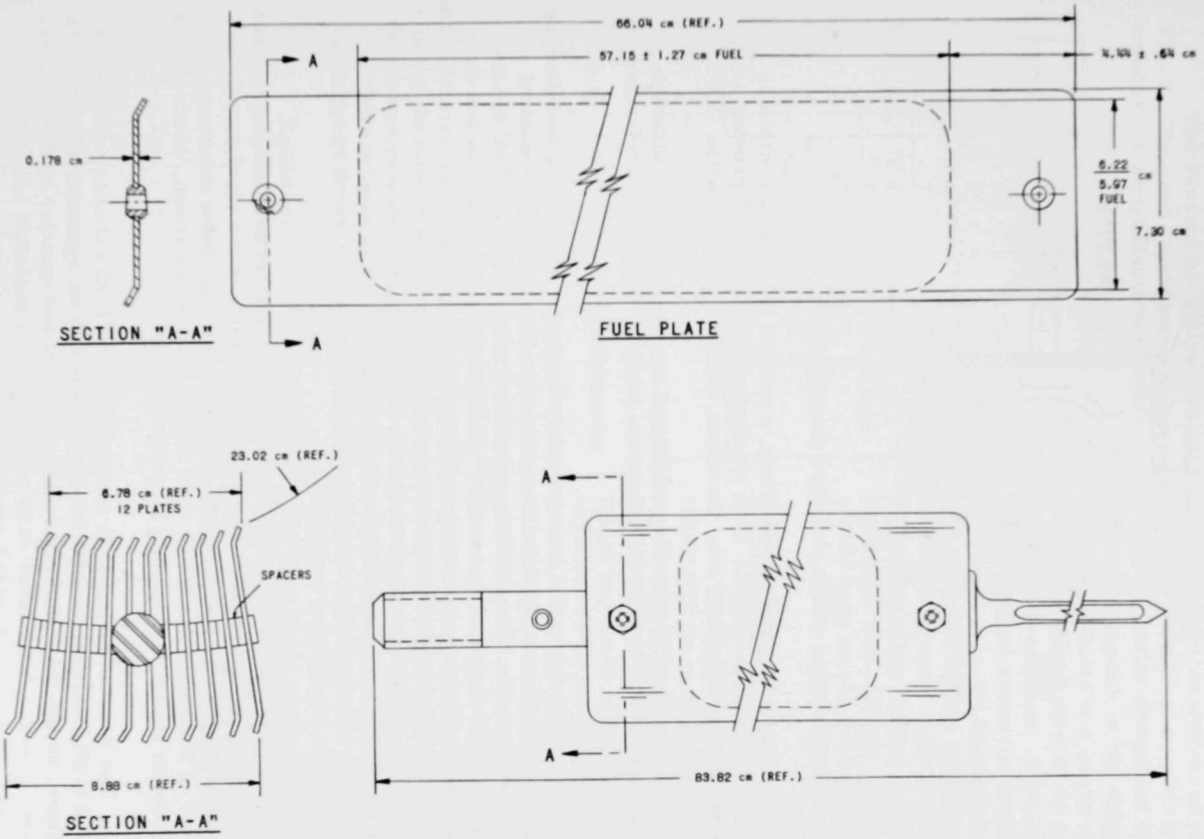

Fig. 1. JUGGERNAUT Fuel Assembly

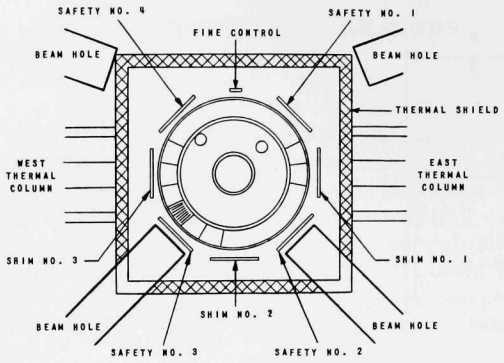

Fig. 2. Core Arrangement

If the spacing is reduced to 0.4207 cm, a total of 280 plates containing 4.9 kg of U^{235} can be loaded. This maximum loading should provide an excess reactivity of 9.5% Δk over the clean, cold, critical condition (3.4 kg).

This method of providing additional excess reactivity, although not as convenient as providing the maximum loading initially, is preferable for 2 reasons:

(1) With the initial configuration, the probability that a fuel-loading error will result in a rapid nuclear excursion is nil, since the control system will be able to maintain a subcritical condition even if all the fuel should be loaded within the core.[12] If the critical experiments had indicated that a greater reactivity margin was necessary than was possible with the initial configuration, the plate spacing would have been reduced in some or all of the assemblies to provide only the minimum necessary reactivity addition. If the maximum fuel-loading configuration had been provided initially, an excess reactivity greater than the total rod worth by approximately 3% Δk would have been possible.

(2) From the standpoint of measuring the effective delayed-neutron fraction (β_{eff}) of the reactor, anything which destroys the ideal symmetry of the core should be discouraged. Hence, one would like a minimum number of dummy plates in the core during the measurement, which means that a lower initial fuel loading is preferable.

The reactor dimensions assumed for the PDQ calculations are indicated in Fig. 3. The reactor was considered to be symmetrical about its midplane, so the view shows a cross section of one-quarter of the reactor.

The reactor as designed differs slightly from that portrayed in Fig. 3. The lead is arranged in a square annulus instead of a cylindrical annulus for simplification in construction. The material designated as concrete-graphite in the diagram actually consists of a heavy-concrete biological shield pierced by 2 graphite thermal columns. Also, the reactor is not exactly symmetrical with respect to the horizontal axis. The extent of the top reflector is somewhat greater than shown and the extent of the bottom reflector somewhat less. These differences should have an almost negligible effect on the critical mass.

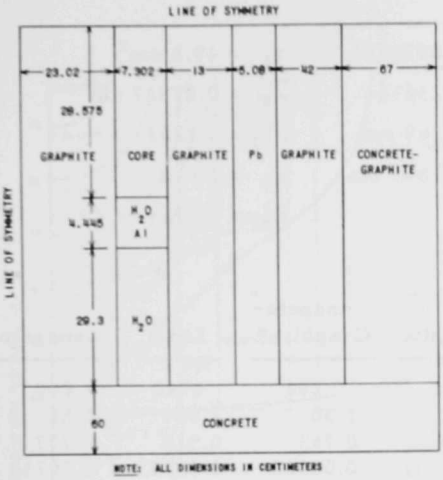

Fig. 3. Idealized Reactor Structure

Two-group Constants

The constants for the JUGGERNAUT were obtained in the same manner as those for the ARGONAUT.[2] Initially, no attempt was made to include the variation of the fission and absorption cross sections with radius within the core. The dimensions used for the core were the "active" length and width. In the vertical direction this included only that part of the fuel plate containing U^{235}. The aluminum ends were included in a separate reflector region distinct from the pure H_2O reflector. The total width of the plate was considered active, although this is not strictly true. The aluminum containers and the thin shell of H_2O between them and the core were not included in the initial machine calculations. The reactivity effect of these shells was first evaluated by perturbation methods and later by diffusion calculations.

Epithermal effects on the fission and absorption cross sections, although small, were included by using Westcott's[8] formalism, in connection with the 1959 World consistent set[7] of cross sections. The effective neutron temperature was found by means of the expression[9]

$$\frac{T_N}{T_M} = 1 + A \frac{\Sigma_a(kT_M)}{\Sigma_s} \quad .$$

Disadvantage factors were obtained from P_3 calculations.

Several different plate spacings were considered. Sets of constants for each plate spacing can be deduced from Table 16. The final design incorporates 12 plates per box for which the constants are given in Table 5.

Table 5

JUGGERNAUT TWO-GROUP CONSTANTS

Core

T_M = 20°C	$f_{U^{235}}$ = 0.002293[9]	τ_f = 49.8 cm^2
T_N = 40°C	f_{Al} = 0.25234	$\overline{\Sigma}_a$ = 0.07827 cm^{-1}
$W_{U^{25}}$ = 3.0 kg	D_1 = 1.269 cm	$\nu\overline{\Sigma}_f$ = 0.1262
f_{H_2O} = 0.74537	D_2 = 0.1863 cm	k_∞ = 1.612
		B_m^2 = 0.0114

Reflector

	H_2O-Al	H_2O	Graphite	Concrete-Graphite*	Lead	Concrete
τ_f (cm^2)	59.8	31.8	385	244	4740	205
D_1 (cm)	1.33	1.20	1.14	1.36	1.684	1.51
D_2 (cm)	0.231	0.142	0.916	0.765	0.918	0.707
Σ (cm^{-1})	0.0167	0.0195	0.000367	0.00503	0.00503	0.00736

*Assumed to be one-third graphite, two-thirds concrete (atom density).

Adjoint* and Real Fluxes

Figures 4 to 7 show the lines of intersection of surfaces of constant flux with either bottom quadrant of any diametral plane cut vertically through the core. The surfaces of constant flux are symmetrical with respect to the core midplane. The adjoint and real fluxes were obtained by means of the PDQ code and the assumption of a 3.5-kg U^{235} loading and all control rods withdrawn.

The values shown for the adjoint fluxes (see Figs. 6 and 7) are such that

$$\int_{\text{core}} \Sigma_{a_2} \phi_1^+ \phi_2 \, dV = 1.455 \times 10^{17} \quad ,$$

where the values for ϕ_2 are obtained from Fig. 4.

Radial and vertical thermal-flux shapes are shown in Figs. 8 and 9.

*See Appendix B.

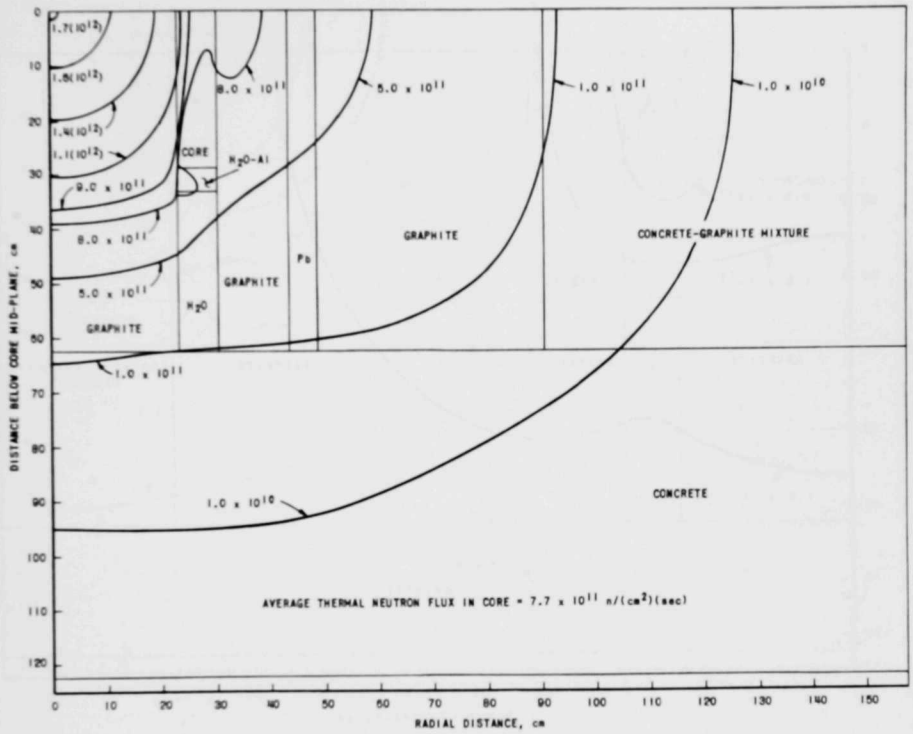

Fig. 4. Thermal-neutron Flux at 100 kw with All Control Rods Withdrawn

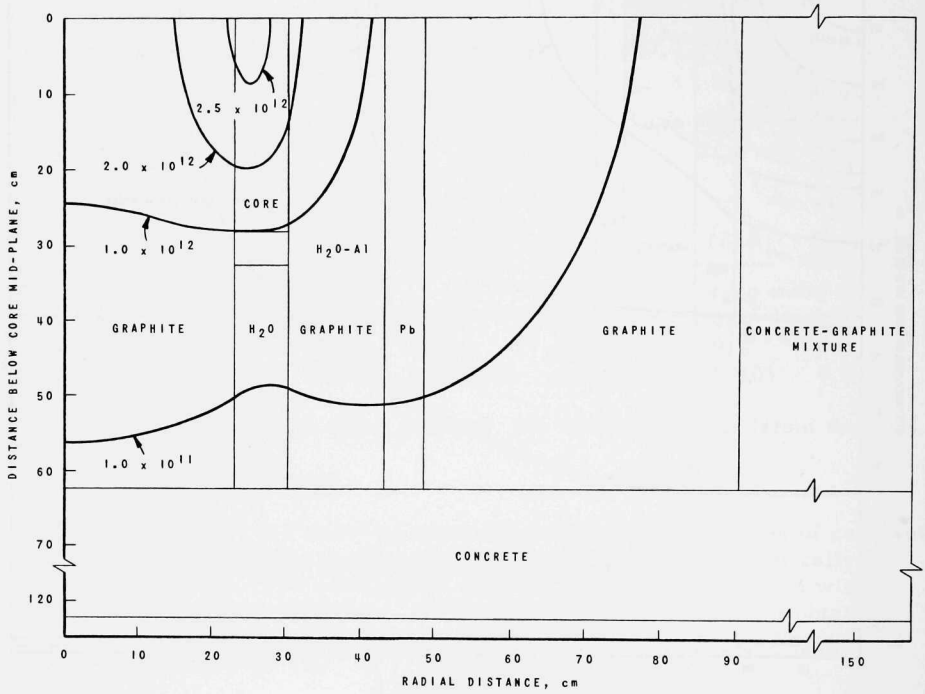

Fig. 5. Fast-neutron Flux at 100 kw with All Control Rods Withdrawn

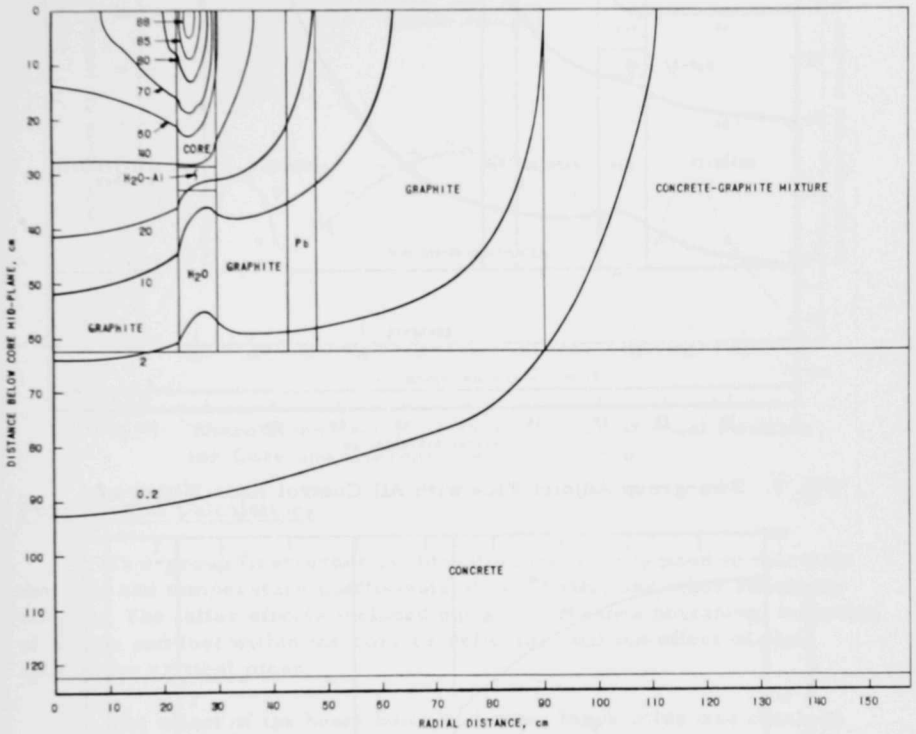

Fig. 6. Two-group Thermal Adjoint Flux with All Control Rods Withdrawn

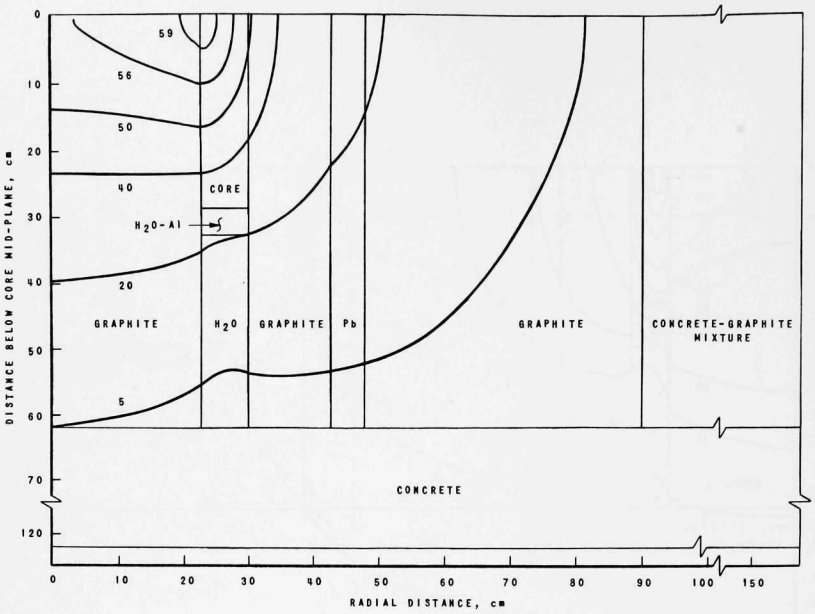

Fig. 7. Two-group Adjoint Flux with All Control Rods Withdrawn

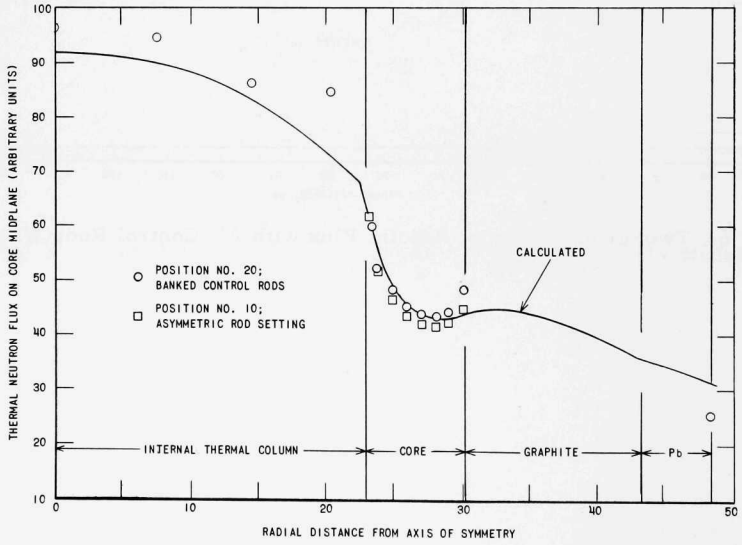

Fig. 8. Thermal-neutron Flux as a Function of Radial Position at Core Midplane

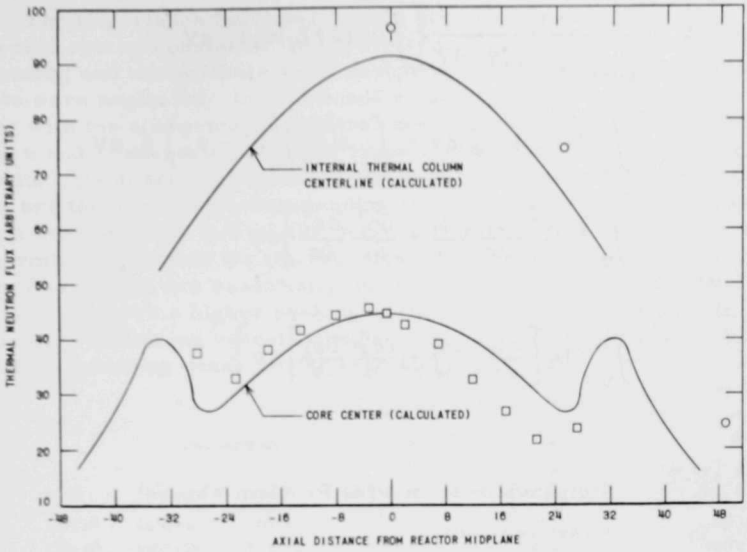

Fig. 9. Thermal-neutron Flux as a Function of Axial Position for Core and Internal Thermal Column

Perturbation Calculations

Two-group first-order perturbation theory was used to calculate the void and temperature coefficients of reactivity, and other reactivity effects. The latter effects included equilibrium xenon poisoning, insertion of poison and fuel within the core or reflector, and the effect of plate spacing on critical mass.

The effect of the beam holes and other large voids was obtained from an empirical relationship, involving the adjoint and real fluxes, which is in good agreement with experimental data from a variety of reactors.[4]

The change in reactivity ($\Delta\rho$) effected by small perturbations in the nuclear constants over a volume V was calculated by means of the following system of equations:

$$\Delta\rho \equiv \frac{\overline{\Delta k}}{k^*_\infty + \overline{\Delta k}} \quad ; \tag{1}$$

$$k^*_\infty = \left(\nu^* \frac{\overline{\Sigma}_f}{\overline{\Sigma}_a}\right)_{core} = \left(\frac{\nu}{\lambda} \frac{\overline{\Sigma}_f}{\overline{\Sigma}_a}\right)_{core} \quad ; \tag{2}$$

$$\overline{\Delta k} = \frac{1}{\int_{core} \Sigma_{a2}\ \phi_1^{\dagger}\phi_2\ dV} \left\{ \int_V \delta(\nu^*\Sigma_f)\phi_2\phi_1^+\ dV \right.$$

$$- \int_V \delta(\Sigma_a)\phi_2\phi_2^+\ dV - \int_V \delta\left(\frac{D_1}{\tau}\right)\left(\phi_1^+ - \phi_2^+\right)\phi_1\ dV$$

$$- \int_V \delta D_1 \left[\frac{\partial\phi_1^+}{\partial r}\frac{\partial\phi_1}{\partial r} + \frac{\partial\phi_1^+}{\partial z}\frac{\partial\phi_1}{\partial z} \right] dV$$

$$\left. - \int_V \delta D_2 \left[\frac{\partial\phi_2^+}{\partial r}\frac{\partial\phi_2}{\partial r} + \frac{\partial\phi_2^+}{\partial z}\frac{\partial\phi_2}{\partial z} \right] dV \right\} \quad , \tag{3}$$

where

λ = eigenvalue from PDQ Problem $\approx k_{eff}$

ϕ_1 = fast real flux

ϕ_2 = thermal real flux

ϕ_1^+ = fast adjoint flux

ϕ_2^+ = thermal adjoint flux

$\delta(\nu^*\Sigma_f)$ = change in the product: (average number of neutrons released per fission)(fission cross section), for the just critical reactor.

$\delta(\Sigma_a)$ = change in thermal absorption cross section

$\delta(D_1/\tau)$ = change in the fast removal cross section

δD_1 = change in fast diffusion coefficient

δD_2 = change in thermal diffusion coefficient.

In order to evaluate the integrals in Eq. (3), the core was divided into 40 regions (5 radially and 8 vertically). In each region the real and adjoint neutron fluxes were assumed constant and equal to their average values. The average values are part of the output from the PDQ Code.

An analysis of the accuracy of 2-group perturbation theory for the MTR has shown it to be accurate within one part in 10 for a uniform change in any one constant of 15% or less.(11) The inaccuracies arise from changes in the real and adjoint fluxes as the constants change. The fluxes in the JUGGERNAUT should remain approximately constant for all the perturbations analyzed except for the insertion of fuel boxes or H_2O in the internal thermal column.

The importance functions for the core were evaluated with 2 different sets of constants. In the first evaluation a standard operational fuel loading and temperature were assumed. The aluminum containing vessels were neglected. In the second evaluation, a cold critical fuel loading with the aluminum containers taken into account, was assumed. Tables 6 and 7, respectively, show these 2 sets of importance functions. The values given are for regions in the lower one-half of the core; the values are the same for corresponding regions in the upper half. The regions are identified in Fig. 11. A comparison of the radial shape of the thermal adjoint flux for the two cases is shown in Fig. 10. The fast-adjoint flux shapes are essentially identical in the 2 cases. The real thermal flux shows a higher peaking in the external reflector for the case in which the containing vessel is neglected than is shown in Fig. 8, for which the containing vessels have been included.

Table 6

CORE IMPORTANCE FUNCTIONS FOR STANDARD OPERATING REACTOR

Region	$\int dV$	$\int \phi_1^+ \phi_2 dV$	$\int \phi_2^+ \phi_2 dV$	$\int \phi_1 (\phi_2^+ - \phi_1^+) dV$	$\int \left(\frac{\partial \bar{\phi}_1}{\partial r} \frac{\partial \bar{\phi}_1^+}{\partial r} + \frac{\partial \bar{\phi}_1}{\partial z} \frac{\partial \bar{\phi}_1^+}{\partial z} \right) dV$	$\int \left(\frac{\partial \bar{\phi}_2}{\partial r} \frac{\partial \bar{\phi}_2^+}{\partial r} + \frac{\partial \bar{\phi}_2}{\partial z} \frac{\partial \bar{\phi}_2^+}{\partial z} \right) dV$
2	1.53×10^3	0.6290×10^7	0.9133×10^7	0.7754×10^7	0.03×10^3	-88.08×10^3
3	1.74×10^3	0.6277×10^7	0.9105×10^7	0.7630×10^7	3.58×10^3	-66.21×10^3
4	1.74×10^3	0.4586×10^7	0.6621×10^7	0.5244×10^7	11.15×10^3	-52.60×10^3
5	1.22×10^3	0.2201×10^7	0.3043×10^7	0.1745×10^7	14.87×10^3	-34.60×10^3
6	1.62×10^3	0.5546×10^7	0.8350×10^7	0.9185×10^7	1.47×10^3	$+0.66 \times 10^3$
7	1.85×10^3	0.5508×10^7	0.8289×10^7	0.9058×10^7	5.29×10^3	$+2.16 \times 10^3$
8	1.85×10^3	0.3933×10^7	0.5906×10^7	0.6271×10^7	13.14×10^3	$+4.90 \times 10^3$
9	1.29×10^3	0.1851×10^7	0.2647×10^7	0.2063×10^7	17.25×10^3	$+0.22 \times 10^3$
10	1.71×10^3	0.5277×10^7	0.7952×10^7	0.9314×10^7	9.17×10^3	$+8.94 \times 10^3$
11	1.96×10^3	0.5229×10^7	0.7878×10^7	0.9191×10^7	12.94×10^3	$+10.54 \times 10^3$
12	1.96×10^3	0.3707×10^7	0.5547×10^7	0.6367×10^7	18.80×10^3	$+11.29 \times 10^3$
13	1.36×10^3	0.1729×10^7	0.2468×10^7	0.2065×10^7	19.05×10^3	$+3.11 \times 10^3$
14	1.81×10^3	0.5207×10^7	0.7587×10^7	0.8158×10^7	22.10×10^3	$+0.58 \times 10^3$
15	2.07×10^3	0.5167×10^7	0.7527×10^7	0.8045×10^7	25.40×10^3	$+0.87 \times 10^3$
16	2.07×10^3	0.3682×10^7	0.5348×10^7	0.5560×10^7	26.70×10^3	$+0.68 \times 10^3$
17	1.44×10^3	0.1720×10^7	0.2368×10^7	0.1775×10^7	20.40×10^3	-3.95×10^3
18	1.90×10^3	0.5407×10^7	0.7044×10^7	0.5034×10^7	38.87×10^3	-73.00×10^3
19	2.17×10^3	0.5392×10^7	0.7018×10^7	0.4949×10^7	41.66×10^3	-77.32×10^3
20	2.17×10^3	0.3923×10^7	0.5074×10^7	0.3364×10^7	37.17×10^3	-70.63×10^3
21	1.51×10^3	0.1866×10^7	0.2285×10^7	0.0995×10^7	21.70×10^3	-51.73×10^3
Totals (1/2 core)	34.97×10^3 cm^3	8.450×10^7	12.12×10^7	11.38×10^7	3.61×10^5	-4.74×10^5

$k^*_\infty = 1.593$

$W_{U^{235}} = 3.5$ kg

$T_m = 65^\circ C$

$\lambda = 1.0505$

$\int \Sigma_{a2} \phi_1^+ \phi_2 \, dV = 0.6912 \times 10^7$

$\frac{\int_{core} \phi_2 \, dV}{\int_{core} dV} = 49.8$

Table 7

CORE IMPORTANCE FUNCTIONS FOR COLD CLEAN CRITICAL REACTOR

Region	$\int \phi_1^+ \phi_2 \, dV$	$\int \phi_2^+ \phi_2 \, dV$	$\int \phi_1 (\phi_2^+ - \phi_1^+) \, dV$	$\int \left(\frac{\partial \bar{\phi}_1}{\partial r} \frac{\partial \bar{\phi}_1^+}{\partial r} + \frac{\partial \bar{\phi}_1}{\partial z} \frac{\partial \bar{\phi}_1^+}{\partial z} \right) dV$	$\int \left(\frac{\partial \bar{\phi}_2}{\partial r} \frac{\partial \bar{\phi}_2^+}{\partial r} + \frac{\partial \bar{\phi}_2}{\partial z} \frac{\partial \bar{\phi}_2^+}{\partial z} \right) dV$
2	0.4364 x 10^7	0.6209 x 10^7	0.4303 x 10^7	0.18 x 10^3	-59.00 x 10^3
3	0.4315 x 10^7	0.6135 x 10^7	0.4212 x 10^7	2.53 x 10^3	-58.67 x 10^3
4	0.3067 x 10^7	0.4345 x 10^7	0.2843 x 10^7	7.32 x 10^3	-43.99 x 10^3
5	0.1376 x 10^7	0.1868 x 10^7	0.0912 x 10^7	10.46 x 10^3	-21.13 x 10^3
6	0.3887 x 10^7	0.5814 x 10^7	0.5354 x 10^7	0.88 x 10^3	- 1.46 x 10^3
7	0.3826 x 10^7	0.5721 x 10^7	0.5244 x 10^7	3.41 x 10^3	- 0.26 x 10^3
8	0.2668 x 10^7	0.3981 x 10^7	0.3564 x 10^7	8.44 x 10^3	+ 2.41 x 10^3
9	0.1169 x 10^7	0.1660 x 10^7	0.1127 x 10^7	12.44 x 10^3	+ 1.23 x 10^3
10	0.3689 x 10^7	0.5538 x 10^7	0.5464 x 10^7	6.41 x 10^3	+ 8.48 x 10^3
11	0.3625 x 10^7	0.5441 x 10^7	0.5352 x 10^7	8.77 x 10^3	+ 8.75 x 10^3
12	0.2510 x 10^7	0.3761 x 10^7	0.3639 x 10^7	12.22 x 10^3	+ 9.10 x 10^3
13	0.1088 x 10^7	0.1546 x 10^7	0.1133 x 10^7	13.84 x 10^3	+ 3.42 x 10^3
14	0.3565 x 10^7	0.5159 x 10^7	0.4697 x 10^7	15.61 x 10^3	+ 7.91 x 10^3
15	0.3507 x 10^7	0.5073 x 10^7	0.4594 x 10^7	17.68 x 10^3	+ 8.36 x 10^3
16	0.2438 x 10^7	0.3520 x 10^7	0.3120 x 10^7	17.97 x 10^3	+ 6.75 x 10^3
17	0.1061 x 10^7	0.1448 x 10^7	0.0952 x 10^7	15.08 x 10^3	+ 1.29 x 10^3
18	0.3533 x 10^7	0.4488 x 10^7	0.2614 x 10^7	36.50 x 10^3	-20.25 x 10^3
19	0.3491 x 10^7	0.4431 x 10^7	0.2553 x 10^7	29.71 x 10^3	-22.76 x 10^3
20	0.2471 x 10^7	0.3121 x 10^7	0.1704 x 10^7	25.09 x 10^3	-24.48 x 10^3
21	0.1100 x 10^7	0.1313 x 10^7	0.0470 x 10^7	16.00 x 10^3	-19.30 x 10^3
Totals	5.675 x 10^7	8.057 x 10^7	6.385 x 10^7	2.605 x 10^5	- 2.136 x 10^5

k_∞ = 1.600

W_{U235} = 3.0 kg

T_m = 20°C

λ = 1.0075

$$\int_{core} \Sigma_{a_2} \phi_1^+ \phi_2 \, dV = 0.4442 \times 10^7$$

$$\frac{\int_{core} \phi_2 \, dV}{\int_{core} dV} = 39.6$$

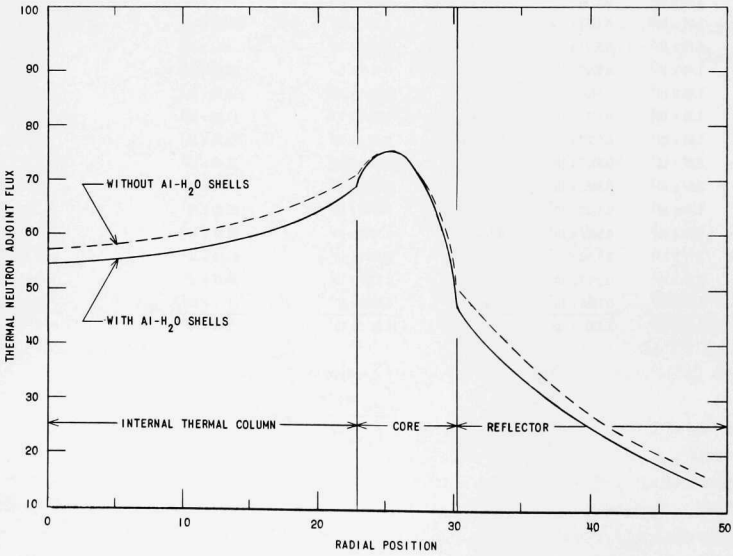

Fig. 10. Comparison of Thermal Adjoint Flux Shapes with and without Al-H_2O Shells Surrounding the Core

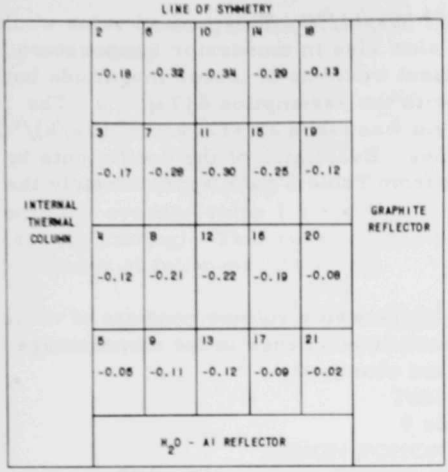

Fig. 11. Local Void Coefficients of Reactivity [%(Δk/k)/1% Void]

Temperature Coefficient of Reactivity

The reactivity effect arising from an increase in moderator temperature is caused not only by changes in the properties of the H_2O moderator but also by the resulting increase in the temperature of the graphite reflector. Since the time constant associated with the increase of graphite temperature is relatively long, this effect should be neglected in the calculation of the prompt temperature coefficient of reactivity. The effect of a non-uniform temperature change on the neutron temperature in the core is not easily analyzed. Hence, the temperature coefficient was calculated by means of 2 different assumptions. These were: (1) the thermal-neutron temperature remains constant; and (2) the neutron temperature varies in direct proportion to T_m.

If any change in the disadvantage factor is neglected, the changes in the 2-group constants (for the cold, clean core) caused by a rise in H_2O temperature from 20°C to 65°C are given in Table 8.

Table 8

CHANGES IN TWO-GROUP CONSTANTS FOR TEMPERATURE RISE OF 45°C

(1) Assuming no change in T_N		(2) Assuming T_N changes with T_M	
$\delta(\nu^*\Sigma_f)$	= 0	$\delta(\nu^*\Sigma_f)$	= -0.00889 cm^{-1}
$\delta(\Sigma_a)$	= -0.000253 cm^{-1}	$\delta(\Sigma_a)$	= -0.005768 cm^{-1}
$\delta(D_1/\tau_f)$	= -0.000404 cm^{-1}	$\delta(D_1/\tau_f)$	= -0.000404 cm^{-1}
$\delta(D_1)$	= +0.025 cm	$\delta(D_1)$	= +0.025 cm
$\delta(D_2)$	= +0.0294 cm	$\delta(D_2)$	= +0.0152 cm

By means of the core importance functions given in Table 7 the effect of these changes was evaluated by use of the equations on page 21. The first assumption results in a total reactivity change of -0.0814% Δk/k, or an average temperature coefficient of -0.18×10^{-4} (Δk/k)/°C. The second assumption results in a total change of -0.932% Δk/k, or an average

temperature coefficient of -2.07×10^{-4} $(\Delta k/k)/°C$. This second value would be the average coefficient for a very slow rise in moderator temperature. For more rapid variation, the coefficient would be of lesser magnitude but would not be as low as that obtained with the assumption $\delta(T_N) = 0$. The average prompt temperature coefficient was taken as -1.5×10^{-4} $(\Delta k/k)/°C$, a rough average between the 2 extremes. Evaluation of the coefficients by means of the core importance functions from Table 6 gave approximately the same result.

Void Coefficient of Reactivity

If it be assumed that 10% of the water volume consists of voids homogeneously distributed and that there is no change in the disadvantage factor, the changes listed in Table 9 are observed.

Table 9

CHANGES IN THE TWO-GROUP CONSTANTS FOR 10% DISTRIBUTED VOIDS

$\delta(\nu^*\Sigma_f) = 0$	$\delta(D_1) = +0.111$ cm
$\delta(\Sigma_a) = -0.00143$ cm^{-1}	$\delta(D_2) = +0.0207$ cm
$\delta(D_1/\tau_f) = -0.003036$ cm^{-1}	

By use of the core importance functions from Table 7 a total reactivity change of -0.0147 $\Delta k/k$ was obtained, resulting in an average void coefficient of -0.147% $(\Delta k/k)/1\%$ void. The use of the importance functions of Table 6 gave essentially the same result.

Figure 7 shows the change of reactivity for each of 20 regions subject to the assumption that a void volume equal to 1% of the total moderator volume is concentrated in that region and no voids are present elsewhere. Each region has an annular shape.

Steady-state Xenon Poisoning

The absorption cross section of xenon at equilibrium can be expressed as

$$\sum_a^{Xe} = \frac{(y_1 + y_2)\,\Sigma_f^{core}}{1 + \frac{\lambda_{Xe}}{\sigma_{Xe}}/\phi_2} ,$$

where

$(y_1 + y_2) = 0.059$

$\lambda_{Xe}/\sigma_{Xe} = 7.35 \times 10^{12}$ n/(cm^2)(sec) .

A rough analysis of the reactivity effect of the xenon was made by evaluating

$$-\delta\rho \approx \frac{\Sigma_a^{Xe}}{\Sigma_a^{core}} = \frac{\Sigma_f^{core}}{\Sigma_a^{core}} \frac{\Sigma_a^{Xe}}{\Sigma_f^{core}}$$

with the average value 1.6×10^{12} n/(cm^2)(sec) for the core thermal flux (4.0-kg loading). This resulted in a reactivity worth of -0.74% $\Delta k/k$ for the xenon at full power (250 kw).

A perturbation calculation was also made to evaluate the effect of the xenon. Table 10 lists the information used in this analysis.

Table 10

XENON POISONING ANALYSIS*

Core Region	$\overline{\phi}_2$ ($\times 10^{-12}$)	$\frac{\lambda_{Xe}}{\sigma_{Xe}}\Big/\overline{\phi}_2$	$\frac{(y_1 + y_2)\,\Sigma_f^{core}}{1 + \frac{\lambda_{Xe}}{\sigma_{Xe}}\Big/\phi_2}$ ($\times 10^3$)	$\int dV \frac{(y_1 + y_2)\,\Sigma_f^{core}}{1 + \frac{\lambda_{Xe}}{\sigma_{Xe}}\Big/\phi_2} \phi_2 \phi_2^+$ ($\times 10^{-4}$)
2	2.24	3.29	0.761	0.695
3	2.10	3.49	0.728	0.663
4	1.82	4.02	0.625	0.430
5	1.62	4.52	0.593	0.180
6	1.88	3.91	0.666	0.556
7	1.75	4.20	0.629	0.521
8	1.49	4.94	0.551	0.325
9	1.30	5.64	0.492	0.130
10	1.74	4.24	0.638	0.507
11	1.62	4.55	0.589	0.464
12	1.36	5.40	0.511	0.283
13	1.18	6.21	0.454	0.112
14	1.69	4.35	0.611	0.464
15	1.57	4.69	0.574	0.432
16	1.33	5.54	0.500	0.267
17	1.16	6.34	0.446	0.106
18	1.75	4.20	0.629	0.442
19	1.65	4.46	0.599	0.420
20	1.42	5.19	0.529	0.268
21	1.26	5.85	0.478	0.109
Total				7.374

*Using importance functions from Table 6.

From the equations on page 21,

$$\rho = \frac{-\int_{core} \frac{(y_1 + y_2)\,\Sigma_f^{core}}{1 + \frac{\lambda_{Xe}}{\sigma_{Xe}}\Big/\phi_2}\,\phi_2\phi_2^+\,dV}{k'\int_{core}\Sigma_{a_2}\,\phi_1^+\phi_2\,dV} = -0.00674 \quad .$$

The xenon worth calculated from perturbation theory is -0.67% $\Delta k/k$, which may be compared with the value of -0.74% $\Delta k/k$ obtained from the simple analysis.

Prompt-neutron Lifetime

From perturbation theory, neglecting slowing-down time, the lifetime is given by

$$\ell = \frac{\int_{\text{whole reactor}} \phi_2\phi_2^+\,dV}{v\int_{core}\nu\Sigma_f\,\phi_2\phi_1^+\,dV} \quad .$$

With the use of the fluxes for the operating reactor, and only roughly approximating these in the reflector region, a lifetime of 2.0×10^{-4} sec was obtained. The lifetime was also evaluated by assuming a uniform addition of poison ($0.0002\ cm^{-1}$) throughout the reactor and obtaining the change in reactivity from the PDQ code.

The lifetime ℓ can then be expressed as(4)

$$\ell = \frac{\frac{\delta\nu}{\nu}\Big/\delta\Sigma_a}{v} = \frac{0.012704/0.0002}{2.705 \times 10^5} = 2.35 \times 10^{-4}\ \text{sec} \quad .$$

The agreement between the methods is satisfactory, particularly since the first method did not take the complete reflector into account.

The effect of inserting the control plates is to reduce the neutron lifetime. If it is assumed that the core is completely surrounded by a thermally black cylinder, the lifetime is calculated (by perturbation methods) to be equal 1.3×10^{-4} sec. With all rods inserted the lifetime would be approximately 1.6×10^{-4} sec.

Effect of H_2O and Aluminum at Core-Graphite Interface

The "active" core width was taken to be the width (7.3 cm) of the fuel plates. It was assumed that a 0.16-cm clearance exists between each vertical core face and the aluminum containing vessels. The outer aluminum container is 0.48 cm thick and the inner is 0.16 cm thick. For calculational simplicity, the aluminum and the thin H_2O shell were homogenized. The resulting mixture was used to replace the graphite which was assumed present in the calculations for the operational core. Table 11 gives the constants for these homogenized shells and their reactivity effect (-2.3% Δk) calculated by perturbation methods.

Table 11

CONSTANTS FOR HOMOGENIZED SHELLS

	Outer Shell	Inner Shell
Al/H_2O	3.0	1.0
Thickness, cm	0.635	0.318
τ_f, cm^2	250	80
D_1, cm	1.64	1.44
Σ_a, cm^{-1}	0.0142	0.0160
D_2, cm	0.512	0.274
Σ_1, cm^{-1}	0.00650	0.0180
Volume,* cm^3	4013	1525
$\delta\Sigma_a$, cm^{-1}	+0.0139	+0.0180
$\delta\Sigma_1$, cm^{-1}	+0.0035	+0.0150
δD_1, cm	+0.53	+0.33
δD_2, cm	-0.404	-0.642
$\int_{shell} \phi_2 \phi_2^+ \, dV$	0.910×10^7	0.680×10^7
$\int_{shell} (\phi_2^+ - \phi_1^+) \, \phi_1 \, dV$	0.296×10^4	0.405×10^7
$\int_{shell} \left(\frac{\partial \phi_1}{\partial r} \frac{\partial \phi_1^+}{\partial r} + \frac{\partial \phi_1}{\partial z} \frac{\partial \phi_1^+}{\partial z} \right) dV$	0.791×10^5	0.824×10^4
$\int_{shell} \left(\frac{\partial \phi_2}{\partial r} \frac{\partial \phi_2^+}{\partial r} + \frac{\partial \phi_2}{\partial z} \frac{\partial \phi_2^+}{\partial z} \right) dV$	-0.325×10^5	-0.143×10^5
$\delta k/k'$, %	-1.58	-0.66
	-2.24	

*Volume is for shell length of 66 cm.

By means of the same constants, the reactivity effect of the shells was calculated, with the PDQ diffusion code, to equal -2.0% Δk. The agreement between the 2 calculations is satisfactory.

Core Inhomogeneity

In all previous calculations the "active" core width has been assumed to be 7.3025 cm. The true active width of the fuel, however, is a nominal 6.0325 cm. Another inhomogeneity exists due to the radial arrangement of the fuel plates. This causes a relatively greater density of fuel and aluminum near the central column and a lower density at the outside edge of the core. The reactivity effect of these inhomogeneities was calculated by perturbation theory with the core divided into 5 equally spaced radial zones. The effect arising from the radial arrangement was calculated first; then the additional effect of moving the U^{235} from the core edge toward the core center was included. The changes in the 2-group constants, with a radial fuel-concentration gradient, compared with a totally homogenized core are listed in Table 12. Zone 1 is at the inner core edge, zone 5 at the outer.

Table 12

CHANGES IN TWO-GROUP CONSTANTS† ASSUMING RADIAL FUEL-PLATE ARRANGEMENT

Zone	Subzones	$\delta(\nu^*\Sigma_f)$ (cm^{-1})	$\delta\Sigma_a$ (cm^{-1})	$\delta\Sigma_1$ (cm^{-1})	δD_1 (cm)	δD_2 (cm)
1	2,3,4,5	+0.015432	+0.007288	-0.000340	+0.056	+0.0081
2	6,7,8,9	+0.007267	+0.003431	-0.000140	+0.026	+0.0037
3	10,11,12,13	0	0	0	0	0
4	14,15,16,17	-0.006511	-0.00308	+0.000124	-0.022	-0.0032
5	18,19,20,21	-0.012376	-0.005852	+0.000316	-0.041	-0.0060

†For clean, cold critical core.

Using the importance functions from Table 8, it was found that the effect of the radial fuel-plate arrangement is to give a reactivity increase of +0.28% $\Delta k/k$ over that obtained for the totally homogenized core.

The effect caused by the movement of fuel from the core edges to the center was calculated subject to the assumption that this change does not affect Σ_1, D_1, or D_2 in any of the zones. Table 13 lists the additional changes caused by this movement.

Table 13

CHANGES IN TWO-GROUP CONSTANTS RESULTING FROM U^{235} MOVEMENT FROM EDGES TOWARD CORE CENTER

Zone†	Volume (cm^3)	$\delta(\nu^* \Sigma_f)(cm^{-1})$	$\delta(\Sigma_a)(cm^{-1})$
1a	2.6646×10^3	-0.14066	-0.068495
1a	3.5628×10^3	+0.02756	+0.013422
2	6.6103×10^3	+0.02790	+0.013585
3	6.9933×10^3	+0.02636	+0.012836
4	7.3762×10^3	+0.02499	+0.012169
5a	4.3385×10^3	+0.02525	+0.012298
5b	3.4206×10^3	-0.11285	-0.054952

†Zones 1 and 5 are divided into subzones 1a, 1b and 5a, 5b, respectively. Zones 1a and 5b contain no U^{235}.

The reactivity effect of this perturbation is -1.15% $\Delta k/k$. Hence, the total effect is -1.15 + 0.28 = -0.87% $\Delta k/k$. This is only approximate, since the necessary conditions that the perturbation does not affect the flux is not strictly true in the second case. The above analysis also neglected any change in disadvantage factor.

Disadvantage Factors

The disadvantage factor used in evaluating the 2-group constants for the 240-plate core was 1.027. The correct value from P_3 calculations is 1.0355 (based on a total loading of 4.0 kg instead of 3.0 kg). The effect of having the edges of the plates free of U^{235} is to raise the disadvantage factor to 1.041. The reactivity change resulting from an increase of disadvantage factor from 1.027 to 1.041 is -0.42% $\Delta k/k$.

Although the P_3 method results in too low a value of the disadvantage factor for thin plates, the prediction of critical mass should not be affected, since the P_3 method was used with success in the ARGONAUT calculations. If a higher value for the disadvantage factor were used, its effect could be balanced by a reduction in the neutron age in the core. This trend is favored by recent measurements in light water.

Summary of Important Reactivity Effects

In Table 14 are listed certain important reactivity effects as calculated by perturbation theory for JUGGERNAUT.

Table 14

SUMMARY OF CALCULATED PERTURBATION EFFECTS

Average Void Coefficient of Reactivity	-0.15% $(\Delta k/k)/1\%$ void
Average Temperature Coefficient of Reactivity (20°C to 65°C)	-0.20% $(\Delta k/k)/°C$
Average Prompt Temperature Coefficient of Reactivity (20°C to 65°C)	-0.015% $(\Delta k/k)/°C$
Prompt Temperature Coefficient of Reactivity (65°C)	-0.019% $(\Delta k/k)/°C$
Average Prompt Neutron Lifetime (3.0 kg Loading)	2.3×10^{-4} sec
Effect of Equilibrium Xenon at 250 kw	-0.67% $\Delta k/k$
Effect of 15-cm Beam Hole Ending at Core Face	-0.36% $\Delta k/k$
Effect of 15-cm Beam Hole Ending Outside Lead	-0.10% $\Delta k/k$
Removal of Central 15-cm Graphite Plug	-2.4% $\Delta k/k$
Replacing Central 15-cm Graphite Plug with H_2O	-4.4% $\Delta k/k$
Insertion of One Fuel Box into Air-filled Central Hole	+3.6% $\Delta k/k$ max.
Insertion of One Fuel Box into H_2O-filled Central Hole	+3.2% $\Delta k/k$ max.
Worth at Center of Internal Thermal Column of:	
U^{235}	+0.030% $(\Delta k/k)/gm$
Cadmium	-0.009% $(\Delta k/k)/cm^2$
Dilute Poison	-0.0363 $(\Sigma_a V)\% \Delta k/k$
Void	$-0.62 \times 10^{-5}\%$ $(\Delta k/k)/cm^3$
H_2O	$-0.47 \times 10^{-3}\%$ $(\Delta k/k)/cm^3$
Flooding Control Thimbles with H_2O	-0.12% $(\Delta k/k)$/thimble
Homogeneous Addition of U^{235} to Core	+0.0078% $(\Delta k/k)/gm$
Worth of Natural Uranium Fission Plate (30 cm sq, 2.5 cm thick) Outside Reflector	$<$+0.15% $\Delta k/k$
Effect of Individual Control Plate Void	-0.036% $\Delta k/k$

Criticality Study

After the plate dimensions had been chosen, the effect of variation of plate spacing on the critical mass was determined from perturbation calculations. The fluxes (see Table 6) for the case of 12 plates per box were used for all spacings. Table 15 summarizes the core characteristics for each of the plate spacings investigated. Figure 12 shows the variation of k_{eff} as a function of H/U^{235}.

Table 15

VARIATION IN CORE PROPERTIES FOR DIFFERENT PLATE SPACINGS

Number of Plates per Box	Average Plate Spacing (cm)	H/U^{235} Atom Ratio	$\delta(\nu\Sigma_f)$ (cm^{-1})	$\delta(\Sigma_a)$ (cm^{-1})	$\delta\left(\frac{D_1}{\tau}\right)$ (cm^{-1})	$\delta(D_1)$ (cm)	$\delta(D_2)$ (cm)	$\delta k/k'$
8	0.8696	425	-0.00378	-0.00131	+0.002266	-0.032	-0.0197	+0.90%
10	0.6601	403	-0.00124	-0.000331	+0.001208	-0.017	-0.0103	+0.67%
12	0.5205	381	0	0	0	0	0	0
14	0.4207	360	+0.00093	+0.000266	-0.001197	+0.016	+0.0113	-0.84%

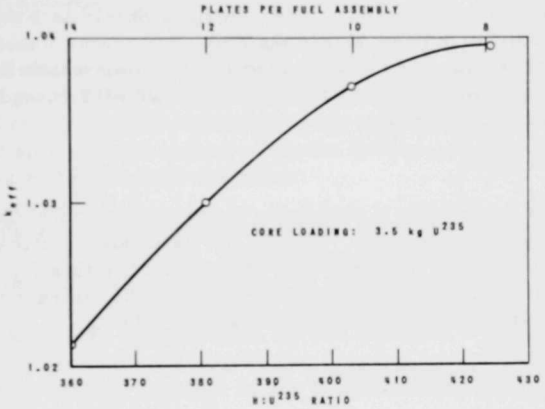

Fig. 12. Variation in Reactivity with $H:U^{235}$ Ratio as Effected by Number of Plates per Assembly

The plate spacing chosen (12 plates per box) provided a slightly undermoderated core, hence giving a relatively large negative void coefficient of reactivity while not departing significantly (0.1 kg) from a condition of minimum critical mass. The use of close plate spacing is also favored from the standpoint of reactor safety.(12) This plate spacing limits the maximum loading to 4.2 kg U^{235}. If additional reactivity should be needed, the maximum loading can be increased to 4.9 kg by reducing the plate spacing (see page 14).

The critical mass for a number of different reactor conditions was predicted by taking all perturbation effects into account. The basis for these predictions was the calculation for the cold clean reactor with a fuel loading of 3.0 kg which showed an excess reactivity of +0.747%. This calculation included the effect of the Al-H_2O shells surrounding the core.

The perturbation effects for the cold clean core (3.0-kg loading) which were taken into account are listed below:

		%Δk
(1)	Excess Reactivity of Homogenized Core	+0.75
(2)	Effect of Core Inhomogeneities	-0.87
(3)	Effect of Disadvantage Factor Correction	-0.42
(4)	Effect of Control Plate Voids	-0.25
(5)	Effect of Overflow Pipe (located in graphite reflector)	-0.4
(6)	Effect of Gap (0.15 cm) between Core and Reflector	-0.5
(7)	Effect of Steel in Beam Tubes	-0.3
(8)	Effect of Steel Liners inside Concrete Shield	-1.0
(9)	Effect of Steel Pedestal for Lead Thermal Shield	-0.6
(10)	Correction Because Lead Thermal Shield is Further from Core Than Was Assumed	+0.6
(11)	Correction for Geneva-type Fuel Plates which Result in a Lower Critical Mass for ARGONAUT than did the Older Type Plate	+0.8
	Total	-2.2

In order to provide a reactivity increment of 2.2% Δk, 0.3 kg of U^{235} must be added to the core. Hence, the estimated critical mass is 3.3 kg U^{235}. No detailed error analysis was performed for this figure, but based on past experience it was believed that it should be correct to within ±0.2 kg. The experimental critical mass was 3.38 kg.

Delayed-neutron Fraction

The effective delayed-neutron fraction for the JUGGERNAUT was calculated with 3 energy groups by the PDQ code. The fast-group constants for both a prompt- and a delayed-neutron spectrum were obtained from MUFT by use of the consistent B_1 approximation. To obtain the correct source shape, a PDQ problem utilizing the group constants for the prompt spectrum was run. The converged fluxes were then used for the flux guess in a new problem utilizing the group constants for the delayed-neutron spectrum. The ratio of the eigenvalue λ after one outer iteration to the converged eigenvalue from the initial problem is just equal to β_{eff}/β. The value obtained was

$$\beta_{eff}/\beta = \frac{1.198}{1.0275} = 1.166 \quad .$$

If $\beta = 0.0064$, then $\beta_{eff} = 0.0075$.

For a critical bare reactor with the same core properties and same value of B_m^2, the effective delayed-neutron fraction by age theory is 0.0087, and by a two-group analysis 0.0080. The effective delayed-neutron

fraction for the JUGGERNAUT is lower than that predicted by a bare core analysis because it has a high-leakage core surrounded by a good thermal reflector. The preferential leakage of prompt neutrons from the core is not as important since a significant fraction of these neutrons return to the core, and the return probabilities do not differ greatly for the 2 neutron species.

The constants obtained from MUFT result in a 2% gain in reactivity compared with the constants given in this report for the reference core. The thermal constants were the same in each case.

Control System Design

A combined shim-safety system consisting of 7 boron-steel plates is used for control. At least 4 of these rods must be completely withdrawn during reactor operation; hence they act as safety rods. The vertical positions of the other 3 rods are indicated at the control panel. The 7 shim-safety plus one fine control rod are equally spaced around the perimeter of the core within the graphite reflector.

The rods are located external to the core to allow a simple core design and fuel-loading scheme. In addition, movement of the control rods causes a minimum of flux perturbation in the internal thermal column, while at the same time not interfering significantly with the external experimental facilities. Boron-steel (0.282 cm thick) is used as the control material to eliminate any possibility that the rods would melt if an accidental Wigner energy release in the graphite were to occur.

The design of the control system was based on the following requirements:

(a) a total shim worth of approximately 4% Δk;

(b) a cold shutdown margin of approximately 3% Δk with water in the core;

(c) any single rod worth no more than \$2 (~1.5% Δk), and

(d) four-rod shutdown at any time.

To operate for 2 yr at 250 kw (0.55 load factor) with no refueling would require an initial excess reactivity (compared to cold critical reactor with beam holes open) of 3.4% Δk and, hence, a shim system worth of the same magnitude. After the samarium has reached a equilibrium concentration, a shim system worth of only 1.8% would be necessary to ensure fuel addition no more than once a year. The remainder of the shim system would be available to compensate for experimental changes.

In order to avoid certain design problems, the total travel of each control rod was limited to approximately 50 cm.[11] For this reason, the rods extend from the top of the core to 18.4 cm below the core centerplane when fully inserted. Since the top shield plug has a greater outside diameter than does the core, it was necessary to incline the control rods at an angle of 5° to the vertical in order to bring them close to the core. Hence, there is no constant separation of control rod and core. A mean distance of 4 cm was initially assumed in all calculations.

In order to determine the individual worth of each rod as a function of its length and width, a series of PDQ problems was analyzed. A number of problems in R-Z geometry were run subject to the assumptions that a variable-width band of cadmium surrounded the reactor and was centered on the core midplane at a distance of 4.0 cm from the core face. From these data, the worth of a cylindrical cadmium shell as a function of shell height was obtained (see Fig. 13). The effect of the control plate width was determined using X-Y geometry with the reactor core represented as a square "annulus" having the same volume and external perimeter as the annular core. Four control plates, of variable width, extended the length of the core; one plate was centered on each of the 4 core faces at a distance of 4.0 cm from the face. The results are shown in Fig. 14.

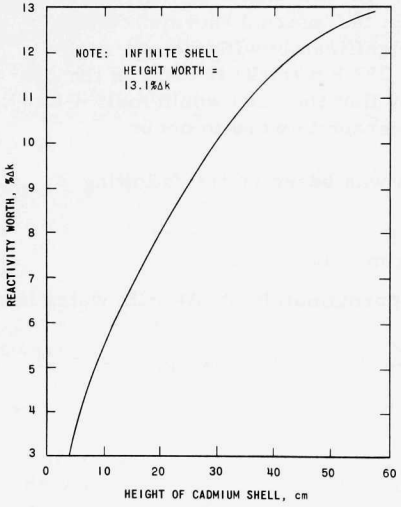

Fig. 13. Worth of Cylindrical Cadmium Shell as a Function of Shell Height

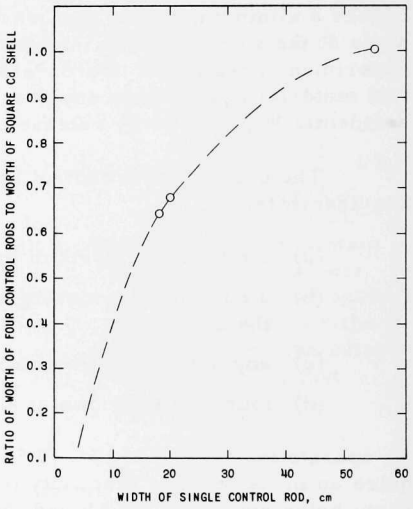

Fig. 14. Worth of Control Rod System Relative to Cadmium Shell

From these 2 sets of problems, the worth of 4 rods of a particular width and height centered at any plane were established. However, to obtain the true worth of a bank of 4 rods, several corrections had to be made. First of all, the effective average distance of the control plates from the core edge (as calculated from perturbation theory) is slightly greater than 4.0 cm. This results in a 10% decrease in the worth of the rods as compared with the results of the PDQ analysis. Also, in the problems utilizing X-Y geometry the plates were placed in positions on the core perimeter of maximum worth. An average rod worth is 10% less than that obtained from these problems. Experiments in the ARGONAUT have indicated that the worth of 2 wt% natural boron in steel plate, 0.282 cm thick, is 0.95 times the worth of cadmium (0.102 cm thick). In these series of problems no Al-H_2O shell around the core was included. From the results of later problems it was found that the ratio of the thermal-neutron importance at the rod position with the shell present to that without the shell is equal to 0.83. The overall effect of these 4 corrections can be expressed as a factor, 0.64, by which the rod worths found from the PDQ analysis were multiplied.

The width of each shim-safety rod was selected to be 17.8 cm and the length to be 48.2 cm (extending from 18.4 cm below the core midplane to the top of the core). From the PDQ calculations the worth of a bank of 4 of these rods was determined to be 7.6% Δk. Applying a factor of 0.64 results in a 4-rod worth of 4.86% Δk. One further correction was then necessary. Since the worth of each control plate void relative to graphite was calculated as -0.036% Δk, the worth of the 4-rod bank was reduced by 0.14% Δk to 4.7% Δk. This compares with a measured value of 4.6 $\pm$ 0.3% Δk.* It was also assumed that the worth of a single rod would be equal to one-fourth the worth of the bank of 4 rods, or 1.2% Δk. The experimental values ranged from 0.8% Δk to 1.2% Δk, depending upon the location of the remaining rods. For a banked position of the remaining rods, the worth of an individual rod was 1.05 $\pm$ 0.05% Δk.

The total shutdown effect of the 7 shim-safety rods was calculated by assuming 4 rods to be present with the same total area as if 7 rods had been used. This resulted in a calculated worth of 6.4% Δk for the control system in the cold clean core. The actual worth was determined to be 7.5 $\pm$ 0.3% Δk. If shadowing effects had been neglected, the calculated worth of the shim-safety system would have been 8.2% Δk.

The shim system consists of 3 plates located to the east, south, and west of the core. The assumption that these systems are worth three-fourths of the 4-rod system resulted in a calculated worth of 3.5% Δk compared with a measured worth of 3.7 $\pm$ 0.4% Δk. During normal operation

*Assuming β_{eff} = 0.0075.

the beam holes are open except for prescribed shielding. This does not affect the worth of the shim system significantly but does reduce the worth of 2 of the safety rods by an amount equal to the negative effect of removing graphite plugs from the beam tables. In this situation, the overall worth of the control system is reduced to 7.0% Δk, and the shutdown effect of the 4 safety plates is 3.3% Δk.

The shim rods are located in a region with a maximum unperturbed thermal-neutron flux of 2×10^{12} n/(cm^2)(sec) at an operating level of 250 kw. The safety rods are to be withdrawn to a region with a maximum thermal neutron flux of 1×10^{12} n/(cm^2)(sec). The actual flux at the surface of the rods is a factor of 0.2 times the unperturbed flux. The percentage of B^{10} atoms which will be burned within a shim rod in one year is 1.5%, while the percentage of total atoms in each such rod which would be transmuted is only 0.03% per year.

Growth is not initiated until a total atom transformation of approximately 0.7% is reached. After 10 yr in JUGGERNAUT, the shim rods will have reached a total atom transmutation of only 0.3%, but a B^{10} burnup of 15%. This B^{10} depletion would lead to a 3→4% reduction in the total control system worth, or -0.2% Δk.

Experimental Data

In Table 16 are listed the experimental and calculated values of all the more important reactor parameters and reactivity effects. Rods worths were obtained initially by rod-drop method wherein the flux decay is followed for periods up to 75 sec after the drop and then the worth obtained from precalculated curves of reactivity vs flux ratio of different times after the drop.

Table 16

SUMMARY OF REACTOR PARAMETERS

	Experimental	Calculated
Neutron Flux, n/(cm^2)(sec)		
Thermal (max)	3.8×10^{12}	4×10^{12}
Thermal (core average)	1.51×10^{12}	1.6×10^{12}
Fast (max)	-	7×10^{12}
Fast (core average)	-	5×10^{12}
Minimum Critical Mass, kg U^{235}	3.38	3.3
Fuel Consumption	-	62 gm/yr at load factor = 0.5
Average Void Coefficient of Reactivity, % Δk/% void	-0.13	-0.15
Average Prompt Temperature Coefficient of Reactivity (20°C to 54°C), % Δk/°C	-0.020	-0.015
Delayed Temperature Coefficient of Reactivity, % Δk/°C	+0.006	-
Reactivity Effect of Equilibrium Xenon at 250 kw, % Δk	-	-0.6
Excess Reactivity Controlled by Shim Rods, % Δk	3.7 ± 0.4	3.5
Combined Worth of Shim Safety Rods (4.0 kg loading), % Δk	7.0 ± 0.3	6.0
Effect of 15-cm Beam Hole Ending at the Core Face, % Δk	-0.29	-0.36
Effect of 15-cm Beam Hole Ending Outside Lead, % Δk	-0.02	-0.10
Removal of Central 15-cm Graphite Plug, % Δk	-1.1	-2.4
Replacing Central 15-cm Graphite Plug by H_2O, % Δk	-4.2	-4.6
Homogeneous Addition of U^{235} to the Core, % Δk/gm U^{235}	+0.0078 ± 0.0003	+0.0078

Previous work with the ARGONAUT has confirmed that such a method gives results within 3% of that obtained by period measurements. The total worth of the shim and safety systems were also determined: (1) by a subcritical multiplication method; and (2) by obtaining the worth of the rods in terms of fuel weight and using the fuel worth determined by a period method to obtain the rod worths. The error limits on the rod worths indicate the differences among the methods. All values of reactivity are based upon a calculated value for the delayed-neutron fraction of 0.0075.

Reactivity Requirements

In Table 17 is shown the excess reactivity requirements for 2 yr of operation, at a load factor of 0.55, as a function of operating power. Also included are the total requirements for operation for periods of one year and for 3 months.

Table 17

EXCESS REACTIVITY REQUIREMENTS
(% Δk)

Operating Power (kw)	250	200	150	100
Experimental Apparatus (includes beam holes)	2.1	2.1	2.1	2.1
Xenon Poisoning	0.7	0.5	0.4	0.2
Samarium Poisoning (2 yr at load factor of 0.55)	1.0	1.0	0.9	0.8
Temperature Rise	0.5	0.4	0.3	0.2
U^{235} Burnup (2 yr at load factor of 0.55)	1.2	1.0	0.7	0.5
Totals, Operation for 2 Yr	5.5	5.0	4.6	4.0
Total for One Year of Operation	4.5	4.1	3.7	3.3
Total for Three Months of Operation	3.7	3.3	3.1	2.8

The maximum fuel loading is 4.2 kg U^{235} (170 plates/16.7 gm per plate and 70 plates/20 gm per plate) which will provide an excess reactivity of 6.0% Δk over the cold, clean critical condition (3.4 kg). Upon first going to power, the core was loaded with a full complement of fuel plates (240 plates containing 4040 gm of U^{235}). This would have provided an excess reactivity for the cold, clean reactor of 5.0% Δk. The excess reactivity was reduced to 3.3% Δk by removing the central graphite plug in the internal thermal column plus the graphite plugs for all the beam tables.

Future reactivity additions can be made by replacing one of the assemblies now in the core (containing 202 gm U^{235}) by an assembly containing a somewhat heavier loading (240 gm U^{235}). Six such assemblies are now available, each of which will provide a reactivity gain of 0.3% Δk. Hence, with the fuel available, operation for 5 yr is possible at a load factor of 0.5. Operational lifetime could be extended if this is desired.

APPENDIX A

Optimization of the Internal Thermal Column for the Highest Thermal Neutron Flux

Two-group theory has been used to obtain the radius of the internal thermal column which will give the highest thermal-neutron flux at the center of the column for an idealized cylindrical-shell reactor. The fuel shell is of infinitesimal thickness, but is considered to be black to thermal neutrons. An infinite reflector region of the same material as the internal column surrounds the shell.

There are 2 reasonable methods of normalizing the neutron flux at the center of the internal column. Normalization to one fission neutron emitted per centimeter of shell height per second would correspond to a condition of constant power for a given shell height as the radius is varied. Normalization to one fission neutron emitted per cm^2 of shell area per second corresponds to a constant power density. The optimum radius depends strongly upon the method of normalization. For a reactor in which the power is the limiting criterion, i.e., JUGGERNAUT, the first method is correct. For reactors of higher performance in which the power density is the limiting criterion, the second method is correct.

The 2-group diffusion equation for the internal column (region I) and the reflector (region II) are given below along with certain of the boundary conditions on the flux in each region:

Region I

$$-D_1 \nabla^2 \phi_1 + \Sigma_1 \phi_1 = 0 \quad ; \quad \left.\frac{d\phi_1}{dr}\right]_{r=0} = 0$$

$$-D_2 \nabla^2 \phi_2 + \Sigma_a \phi_2 = \Sigma_1 \phi_1 \quad ; \quad \left.\frac{d\phi_2}{dr}\right]_{r=0} = 0$$

Region II

$$-D_1 \nabla^2 \phi_1 + \Sigma_1 \phi_1 = 0 \qquad \lim_{r \to \infty} \phi_1 = 0$$

$$-D_2 \nabla^2 \phi_2 + \Sigma_a \phi_2 = \Sigma_1 \phi_1 \qquad \lim_{r \to \infty} \phi_2 = 0 \quad .$$

Solving the above set of equations, we obtain

$$\phi_1^I = A I_0 (\kappa_1 r)$$

$$\phi_2^I = C I_0 (\kappa_2 r) + S A I_0 (\kappa_1 r)$$

$$\phi_1^{II} = EK_0(\kappa_1 r)$$

$$\phi_2^{II} = FK_0(\kappa_2 r) + SEK_0(\kappa_1 r) \quad ,$$

where

$$S = \frac{\Sigma_1}{D_2}\frac{1}{\kappa_2^2 - \kappa_1^2} \quad ; \quad \kappa_1^2 = \frac{\Sigma_1}{D_1} \quad ; \quad \kappa_2^2 = \frac{\Sigma_a}{D_2} \quad .$$

Boundary conditions must now be used to obtain the 4 unknowns in the above set of equations.

1) Normalization

A) The total number of neutrons from the shell is $1/(\text{cm})(\text{sec})$.

$$2\pi r_0 D_1 \left.\frac{\partial \phi_1^I}{\partial r}\right]_{r=r_0} - 2\pi r_0 D_1 \left.\frac{\partial \phi_1^{II}}{\partial r}\right]_{r=r_0} = 1 \quad .$$

B) Current density of neutrons from the shell is $1/(\text{cm}^2)(\text{sec})$:

$$D_1 \left.\frac{\partial \phi_1^I}{\partial r}\right]_{r=r_0} - D_1 \left.\frac{\partial \phi_1^{II}}{\partial r}\right]_{r=r_0} = 1 \quad .$$

2) $$\phi_1^I(r_0) = \phi_1^{II}(r_0)$$

Therefore,

$$AI_0(\kappa_1 r_0) = EK_0(\kappa_1 r_0) \quad .$$

3) Black boundary condition for both region I and II at the fuel shell:

Region I

$$\left. -D_2 \frac{\partial \phi_2^I}{\partial r} / \phi_2 \right]_{r=r_0} = 0.469 \quad .$$

Region II

$$\left. -D_2 \frac{\partial \phi_2^{II}}{\partial r} / \phi_2 \right]_{r=r_0} = 0.469 \quad .$$

The curvature of the shell has been neglected in the black boundary condition. Four conditions are available which enable us to solve for the 4 unknowns; 2 other conditions are rejected as not valid or not necessary:

(1) Thermal fluxes equal at the shell. This is not a valid condition since the thermal fluxes in the 2 regions are independent due to the black boundary separating the regions.

(2) A criticality condition is not necessary since the flux shape is independent of this condition. Hence, this condition will determine only the necessary multiplication properties of the fuel shell in order that criticality be obtained.

Solving for the thermal flux in region I at r=0, we obtain

$$\phi_2^I(0) = \left(\frac{\Sigma_1}{D_2}\,\frac{1}{\kappa_1^2 - \kappa_2^2}\right) \frac{\left[\dfrac{D_2\kappa_1 I_1(\kappa_1 r_0) + 0.469\, I_0(\kappa_1 r_0)}{D_2\kappa_2 I_1(\kappa_2 r_0) + 0.469\, I_0(\kappa_2 r_0)} - 1\right]}{2\pi r_0 D_1 \kappa_1 \left[I_1(\kappa_1 r_0) + \dfrac{I_0(\kappa_1 r_0)}{K_0(\kappa_1 r_0)} K_1(\kappa_1 r_0)\right]} \quad .$$

The factor $2\pi r_0$ in the denominator exists because of normalization to one n/cm/sec from the shell. If normalization to one $n/cm^2/sec$ is used instead, this factor is replaced by one.

In order to solve the above for the r_0 at which a maximum thermal flux is reached, $\phi_2^I(0)$ is differentiated with respect to r_0 and the resulting expression is equated to zero. The solution is straightforward.

Implicit in the previous solution is the assumption of an infinite cylinder. If a finite cylinder is assumed, 2 changes are evident. First, κ_1^2 and κ_2^2 change, since the effect of the finiteness of the cylinder can be represented by adding a term $D_i B_z^2$ to the absorption in both the thermal and fast groups. Hence,

$$\kappa_1^2 = \frac{\Sigma_1}{D_1} + B_z^2 \quad ; \quad \kappa_2^2 = \frac{\Sigma_a}{D_2} + B_z^2 \quad .$$

The magnitude of the normalization factor is also affected; however, this does not change the solution.

Figure 15 shows δ vs r_0, where δ is proportional to $d\phi_2^I(0)/d\, r_0$. The r_0 for which δ becomes zero is the optimum radius for maximum thermal-neutron flux subject to the given assumptions. Since the JUGGERNAUT is 60 cm in length and is power limited, the optimum radius of the internal thermal column would seem to be $1.03\sqrt{\tau}$ or 19.5 cm.

Although this is approximately correct, the finite thickness of the fuel shell must be taken into account. This was achieved by solving several 2-group, 3-region calculations in which a thin shell of water of varying thickness was inserted between the internal graphite column and the fuel shell. An optimum column radius was obtained for each thickness

of water shell. Then the optimum radius for an H_2O internal thermal column was compared with experiment. This revealed that the effect of a 7-cm-thick Al-H_2O core could be accounted for by assuming a 1.4-cm-thick shell of H_2O between the internal column and the infinitesimal fuel shell. For this shell thickness it was found that the optimum radius of a graphite internal column is approximately 15 cm.

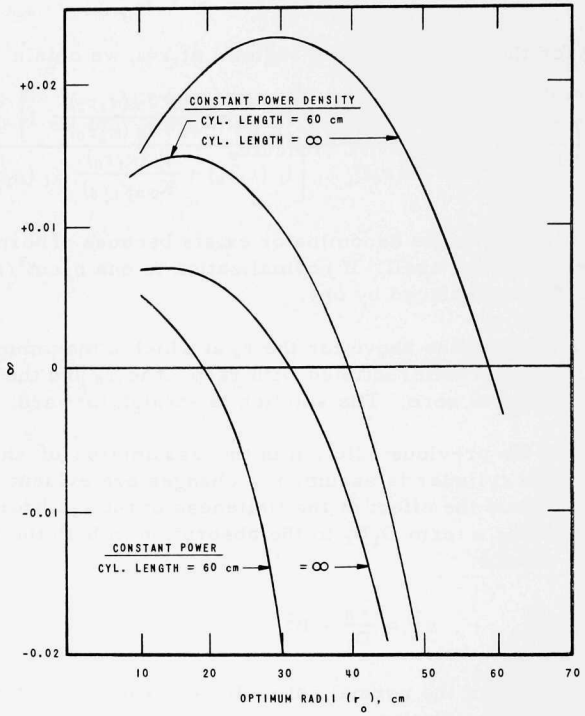

Fig. 15. Optimum Radii of Graphite Internal Thermal Columns

APPENDIX B

Computation of Adjoint Fluxes Using PDQ

By means of the general method of Bertram Wolfe (Nucleonics, March 1958, p. 121) with appropriate modifications due to the peculiarities of the PDQ code, a method of computing the adjoint fluxes by switching input constants has been developed. This method is applicable with 2, 3, or 4 groups, although (with PDQ02) restrictions are necessary which limit the usefulness of this method for epithermal systems which contain different nuclear materials in separate regions. PDQ03 does not require these restrictions. Given below are the 2-group equations and the necessary substitutions which will give the adjoint flux. The extension to 3 or 4 groups is only slightly more difficult.

$$\nabla\cdot D_1\,\nabla\phi_1 - (\Sigma_1^r + \Sigma_1^a + B_z^2\,D_1)\phi_1 + \frac{\nu_1}{\lambda}\,\Sigma_1^f\,\phi_1 + \frac{\nu_2}{\lambda}\,\Sigma_2^f\,\phi_2 = 0$$

$$\nabla\cdot D_2\,\nabla\phi_1 - (\Sigma_2^a + B_z^2\,D_2)\phi_2 + \Sigma_1^r\,\phi_1 = 0$$

$$\nabla\cdot D_2\,\nabla\phi_2^+ - (\Sigma_2^a + B_z^2\,D_2)\phi_2^+ + \frac{\nu_2}{\lambda}\cdot\Sigma_2^f\,\phi_1^+ = 0$$

$$\nabla\cdot D_1\,\nabla\phi_1^+ - (\Sigma_1^a + \Sigma_1^r + B_z^2\,D_1)\phi_1^+ + \frac{\nu_1}{\lambda}\cdot\Sigma_1^f\,\phi_1^+ + \Sigma_1^r\,\phi_2^+ = 0$$

In R-Z geometry, $B_z^2 = 0$.

To obtain the adjoint fluxes

For	Substitute	For	Substitute
ϕ_1	ϕ_2^+	Σ_1^a	$\Sigma_2^a - \Sigma_1^r$
ϕ_2	ϕ_1^+	B_z^2	B_z^2
D_1	D_2	$\nu_1\,\Sigma_2^f$	0
D_2	D_1	$\nu_2\,\Sigma_2^f$	$\nu_2\,\Sigma_2^f$
Σ_1^r	Σ_1^r	Σ_2^a	$\Sigma_1^a + \Sigma_1^r - \frac{\nu_1\,\Sigma_1^f}{\lambda}$

$$x_1 = 1.0 \quad ; \quad x_2 = x_3 = 0 \quad .$$

ACKNOWLEDGEMENTS

The author gratefully acknowledges the aid which frequent discussions with Dr. C. N. Kelber and Dr. R. Avery provided. Preliminary physics calculations provided by Mr. J. F. Fagan were of considerable assistance, and much of the experimental data on the ARGONAUT was obtained with the aid of Dr. W. Sturm.

REFERENCES

1. Daavettila, D., and W. Sturm, ARGONAUT Reactor Databook, ANL-6285 (Jan 1961).

2. Moon, D., Two-dimensional Two-group Calculation of the ARGONAUT One Slab Loading, ANL-6154 (April 1960).

3. Lennox, D. H., and C. N. Kelber, Summary Report on the Hazards of The ARGONAUT Reactor, ANL-5647 (Dec 1956).

4. Kelber, C. N., The Theoretical Physics of the ARGONAUT Reactor, ANL-5710 (May 1957).

5. Deutsch, R. W., Computing 3-group Constants for Neutron Diffusion, Nucleonics 15, 1 (Jan 1957).

6. Hughes, D. J., and R. B Schwartz, Neutron Cross Sections, BNL-325 (Jan 1960).

7. Hughes, D. J., New "World-Average" Thermal Cross Sections, Nucleonics 17, 11 (Nov 1959).

8. Westcott, C. H., Effective Cross Section Values for Well-moderated Thermal Reactor Spectra, CRRP-787 (Aug 1958).

9. Reactor Physics Constants, ANL-5800 (p. 109), 1958.

10. McMurry, H. L., Perturbation Theory and Applications, IDO-16015.

11. Webster, J. W., An Analysis of the Accuracy of Perturbation Theory, IDO-16173 (June 1954).

12. Folkrod, J. R., D. P. Moon, and J. K. Saluja, Summary Hazards Report on the JUGGERNAUT Reactor, ANL-6192 (Feb 1961).